Journal of the Iranian Chemical Society (2020) 17:1627–1634
https://doi.org/10.1007/s13738-020-01882-6

ORIGINAL PAPER

Fabrication and characterization of SiO_2@Fe_3O_4@nanodiamonds for vortex-assisted magnetic solid-phase extraction of lead in cigarette samples prior to FAAS detection

Gulsah Saydan Kanberoglu[1] · Erkan Yilmaz[2,3] · Mustafa Soylak[4,5]

Received: 3 October 2019 / Accepted: 17 February 2020 / Published online: 27 February 2020
© Iranian Chemical Society 2020

Abstract
A novel, speed and accurate vortex-assisted magnetic solid-phase extraction procedure for separation–preconcentration and flame atomic absorption spectrometric determination of lead at trace levels has been proposed. Silica-coated magnetic nanodiamonds (SiO_2@MNDs) as magnetic solid-phase extractor were fabricated and characterized by Fourier transform infrared spectroscopy, X-ray diffraction spectrometry and scanning electron microscopy. Pb(II) could be easily separated from the aqueous solution on the SiO_2@MNDs by using a neodymium magnet. Analytical factors affecting the recoveries of Pb(II) such as pH, adsorbent amount, type and volume of eluent and sample volume were optimized. The preconcentration factor, the precision (RSD %, $n=5$), the limit of detection and the limit of quantification were 5, 5.3%, 40.8 and 135 μg L^{-1}, respectively. The effects of matrix ions have been investigated. The presented extraction method has been applied for the determination of lead in cigarette samples and Bush Branches and Leaves certified reference material. Quantitative recoveries changing from 94 to 106% were obtained for accuracy studies.

Keywords Vortex-assisted magnetic solid-phase extraction · Silica-coated magnetic nanodiamonds · Lead · Flame atomic absorption spectrometry · Cigarette samples

Introduction

Heavy metals can be classified among the most toxic substances. Lead as a cumulative toxicant has adverse effects on the all living organisms and especially on the brain, kidneys and other organs including digestive, reproductive and respiratory systems [1–3]. For the non-smoking general population, the main intake sources of the lead are the dust, dirt and ingestion of food; however, smoking tobacco contributes significantly to the intake of lead [4]. Hence, accurate and sensitive analysis of lead in smoking tobacco samples is an important task for analytical chemists.

The most used instrumental detection methods for lead are flame atomic absorption spectrometry [2], inductively coupled plasma mass spectrometry [5], inductively coupled plasma optical emission spectrometry [6] graphite furnace atomic absorption spectrometry [7] and atomic fluorescence spectrometry [8]. Although among them flame atomic absorption spectrometry (FAAS) can be considered as more easy to use, cheap and fast, the main problems of FAAS analysis are the matrix interferences of foreign ions, low sensitivity and levels of trace analytes generally lower than the detection limit of FAAS [9, 10]. In order to solve these drawbacks, sample preparation and/or preconcentration–extraction techniques are usually required before instrumental detection for analytes of trace levels of lead in food-like complex matrices such as smoking tobacco samples. Solid-phase extraction, solvent extraction, cloud-point extraction, co-precipitation and liquid-phase microextraction methods are widely preferred for the separation and preconcentration

✉ Mustafa Soylak
soylak@erciyes.edu.tr

1 Faculty of Sciences, Department of Chemistry, Van Yuzuncu Yil University, 65080 Van, Turkey

2 Faculty of Pharmacy, Department of Analytical Chemistry, Erciyes University, 38039 Kayseri, Turkey

3 Nanotechnology Research and Application Center (ERNAM), Erciyes University, 38039 Kayseri, Turkey

4 Faculty of Sciences, Department of Chemistry, Erciyes University, 38039 Kayseri, Turkey

5 Technology Research and Application Center (TAUM), Erciyes University, 38039 Kayseri, Turkey

of lead at trace levels [9–13]. Among the above-mentioned methods, nowadays magnetic solid-phase extraction (MSPE) as an innovative approach is the mostly preferred method due to its important advantages such as simple isolation and control of sorbents during adsorption and desorption stages via applying external magnetic field, elimination of the main drawbacks of the time-consuming column-type SPE application by applying different extraction apparatuses such as vortex agitation, ultrasonic irrigation and magnetic stirring, reaching fast adsorption and desorption equilibrium and obtaining high adsorption capacity by using well-designed magnetic sorbents [12–15].

Nowadays, the usage of nanomaterials in MSPE methods has gained popularity. Some of them are graphene (G), graphene oxide (GO), carbon nanotubes (CNTs), nanodiamonds (NDs), metal oxide nanomaterials (SiO_2, TiO_2, ZnO, etc.), nanofibers and polymer-based nanomaterials [15–18]. Among these nanomaterials, carbon-based nanomaterials provided unique advantages for solid-phase extraction applications such as high adsorption capacity, chemical resistivity toward too acidic and basic and studied medium used for several times in the same process, and among the carbon-based nanomaterials, nanodiamonds (NDs) have high surface area of about 450 m^2/g and excellent chemical and mechanical properties. Moreover, the main reason of the widespread usage of nanodiamonds is that NDs are non-toxic [19, 20].

The main problem of the usage of iron oxide-based magnetic nanoparticles as adsorbent is the low resistivity to working conditions such as the use of acidic solution for elution of analytes adsorbed and adjustment of pH in different regions. Modification of the magnetic nanoparticles with SiO_2 nanoparticles is an effective solution to increase the resistivity of magnetic nanoparticles for studied sample medium [21].

In the presented study, SiO_2@MNDs were fabricated, characterized and used as a magnetic solid-phase extractor for the separation–preconcentration of lead at trace levels in cigarette samples prior to their FAAS detection.

Experimental

Instrumentation

The pH values were measured with a Sartorius PT-10 model digital pH meter. A vortex mixer (VWR model, Germany) and an ultrasonic bath (Sonorex) were used for experiments. A Perkin-Elmer AAnalyst 300 atomic absorption spectrometer coupled with microsampling unit was used for the determination of lead. The FTIR spectra were recorded on a Perkin-Elmer Spectrum 400 model Fourier transform infrared spectrometer (Waltham, MA, USA). X-ray diffraction spectrum for the SiO_2@MNDs was taken using a Bruker AXS D8 Advance diffractometer. Scanning electron microscope images were obtained on a LEO 440 SEM with an accelerating voltage of 20 kV. Water used in this work is (18 MΩ cm, resistivity) pure water purified with a Milli-Q system (Millipore, USA).

Chemicals and reagents

All reagents used were of analytical grade. Nanodiamonds < 10 nm particle size (no: 636428-1G) were purchased from Sigma-Aldrich (St. Louis MO, USA). Analytical grades of ferrous sulfate heptahydrate ($FeSO_4{\cdot}7H_2O$), ferric chloride hexahydrate ($FeCl_3{\cdot}6H_2O$), nitric acid (65%), acetone and hydrochloric acid (37%) were obtained from Merck (Darmstadt, Germany). Ammonia solution (35%) was purchased from Riedel-de Haen, Sigma-Aldrich (St. Louis MO, USA). Tetraethoxysilane (TEOS) was obtained from Alfa Aesar (Germany).

Fabrication of silica-coated magnetic nanodiamonds

Co-precipitation known as an effective magnetic nanoparticle production method was used to modify nanodiamonds with magnetic Fe_3O_4 nanoparticles. For this purpose, 3.3 g of $FeCl_3{\cdot}6H_2O$ and 2.2 g of $FeSO_4{\cdot}7H_2O$ were dissolved in 150 mL of distilled water, and 150 mg of nanodiamonds was dispersed in this solution by applying ultrasonic irritation. Then, 20 mL of 25% ammonia solution was added drop by drop to the obtained mixture at 85 °C under Ar atmosphere to prevent oxidation of Fe_3O_4 to Fe_2O_3. The obtained magnetic nanodiamonds (Fe_3O_4@NDs) were separated from solution by applying external magnet via a neodymium magnet, washed with distilled water and ethanol and dried in a vacuum oven at 60 °C. The synthesized Fe_3O_4@NDs particles were again redispersed in 100 mL of ethanol/water/concentrated ammonia mixture (80 mL/20 mL/1 mL) by applying ultrasonic irritation. Then, 0.25 mL of tetraethyl orthosilicate (TEOS) was added dropwise and stirred for 6 h at room temperature, and the synthesized SiO_2@MNDs nanocomposite was washed and dried with same procedure given above prior to use.

Extraction method

One hundred and fifty milligrams of the SiO_2@MNDs was added to 20 mL of model solution containing μg L^{-1} level of Pb(II) ions, 2 mL of pH 6.0 phosphate buffer solution was added to the solution, and the solution was mixed for 2 min on a vortex mixer to facilitate adsorption of the Pb(II) onto the SiO_2@MNDs. Then, the magnetic adsorbent was separated by using a strong neodymium permanent magnet and

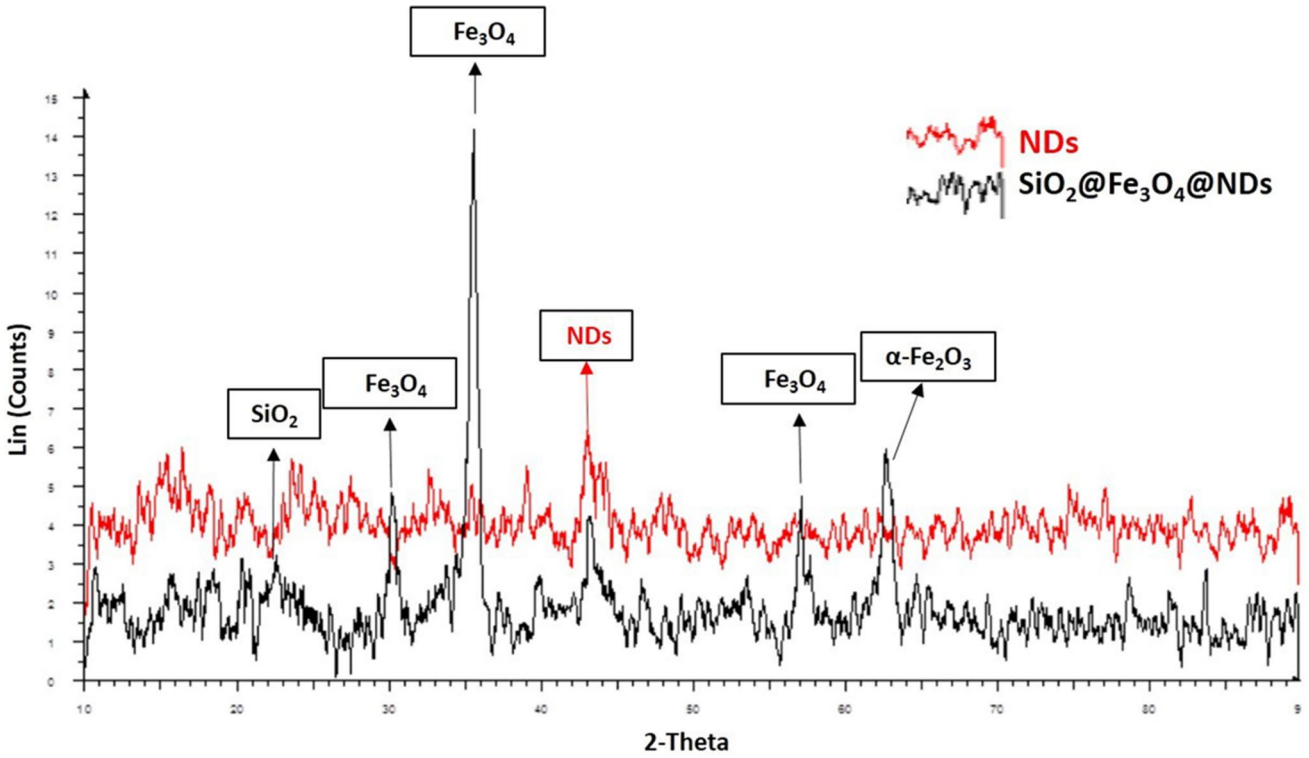


Fig. 1 XRD spectra of the pristine NDs and SiO_2@Fe_3O_4@NDs nanomaterial

the supernatants were decanted directly. Pb(II) ions adsorbed on the SiO_2@MNDs were eluted with 4 mL of 4% thiourea in 1 M HCl solution by applying vortex mixing for 3 min and analyzed by FAAS. The suggested method was also applied for blank samples.

Real sample analysis

Cigarette samples were collected from Kayseri City in Turkey and Bulgaria. The real sample analysis of the developed VAMSPE method for cigarette samples and NCSDC 73349 Bush Branches and Leaves certified reference material was conducted by using same digestion method given in the literature [22]. Ten milliliters from 65% of nitric acid was added to 1.0 g of accurately weighed cigarette sample, and the obtained mixture was evaporated to dryness at 80–90 °C. Later, the same procedure was repeated by the addition of 10 mL of 65% of nitric acid and 5 mL 30% of hydrogen peroxide. After completion of the evaporation of acidic solution, 10–11 mL of distilled water was added to the resulting mixture to extract Pb(II) ions from digested solid phase to water phase and the mixture was filtered through a blue band filter paper. pH was adjusted for an aqueous sample phase and subjected to the developed VAMSPE method explained in Sect. 2.4. The suggested digestion and VAMSPE stages were also applied for blank samples.

Results and discussion

Characterization of SiO_2@MNDs

After the fabrication of SiO_2@MNDs, their magnetic properties were checked by applying external magnetic field. It was seen that whole material was magnetic and completely isolated from an aqueous phase by external magnetic field. XRD spectra of the pristine NDs and SiO_2@MNDs are shown in Fig. 1. Iron oxide species including magnetite (Fe_3O_4), hematite (α-Fe_2O_3), maghemite (γ-Fe_2O_3) and goethite (FeO(OH)) are commonly obtained in the magnetic nanoparticle formation process. Among them, only Fe_3O_4 and γ-Fe_2O_3 bring magnetic features to materials. The SiO_2@MNDs nanomaterial has five main characteristic XRD peaks at $2\Theta = 30.0°$ (220), 35.0° (311) and 57.4° (511) that can be assigned to Fe_3O_4 (JCPDS card no. 19–0629) (Fig. 1) [21]. The broad band $2\Theta = 22.5°$ can be assigned to amorphous silica [23]. The FTIR spectra of pristine NDs and SiO_2@MNDs nanomaterial are illustrated in Fig. 2. When FTIR spectrum of SiO2@MNDs is examined, a characteristic peak at around 566 cm^{-1} belongs to Fe–O bond vibration of Fe_3O_4 nanoparticles. The characteristic bands at 1066, 793 and 462 cm^{-1} are assigned to the stretching, bending and out of plane of Si–O bonds, respectively [23]. SEM and SEM

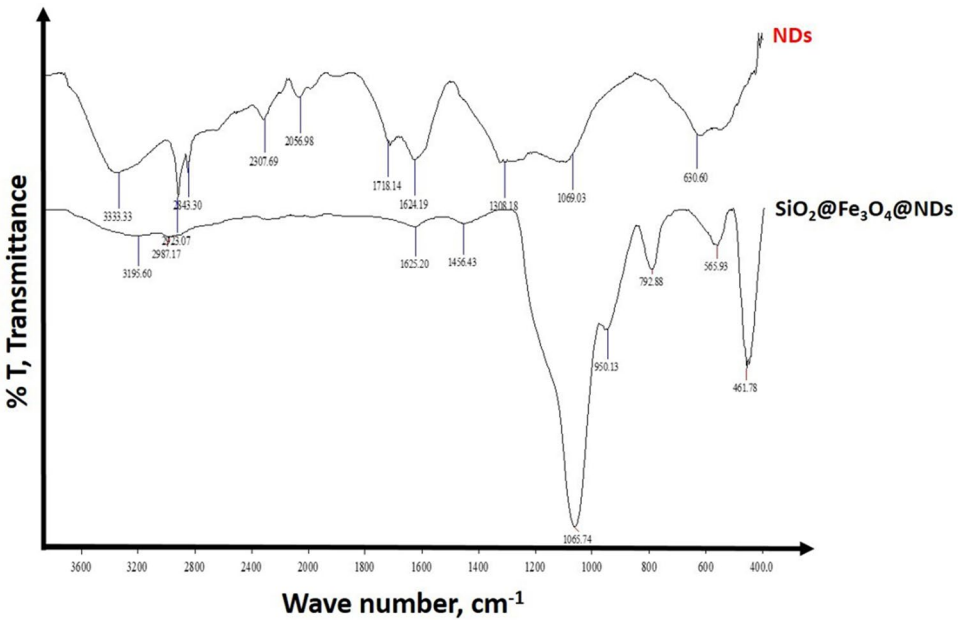


Fig. 2 XRD spectra of the pristine NDs and SiO_2@Fe_3O_4@NDs nanomaterial

mapping analysis results of SiO_2@MNDs are shown in Fig. 3. When compared with SEM images of pristine NDs (Fig. 3a, b), significant changes in surface morphology of the SiO_2@MNDs (Fig. 3c, d) were observed. Moreover, it is seen from mapping analysis that Fe_3O_4 and SiO_2 particles form homogeneously throughout the structure (Fig. 3c, d).

Optimization studies

pH of sample solution is a parameter which has primary impact on the adsorption of the target analytes on the extraction studies, because it was related to the surface charge of the adsorbent as well as the predominant form of analyte species [24–29]. Hence, pH of sample solution should be studied and optimized first parameter. The effect of pH values of the model solutions on the recovery values of lead(II) was investigated in the pH range of 3.0–8.0. The results are depicted in Fig. 4. The recoveries for lead(II) were quantitative in the pH range of 6.0–7.0. For the further works, as the optimum pH, 6.0, was selected.

This situation can be explained by the fact that when pH increases toward alkaline, the surface charge of SiO_2@MNDs became negatively charged and consequently the electrostatic attraction forces between the positively charged Pb(II) ions and the adsorbent surface increase, and as a result, the adsorption increases, but at alkaline pH conditions, $Pb(OH)_2$ is formed and precipitates in the aqueous media and inhibits the adsorption of Pb(II) ions on SiO_2@MNDs surface; hence, for the further works, pH 6.0 was selected as the optimum pH.

Amount of adsorbent used in solid-phase extraction methods is another important parameter, which affects not only the adsorption of analytes but also desorption efficiencies of analytes [30–34]. The influences of the amount of the SiO_2@MNDs as magnetic adsorbent on the recoveries of lead(II) were investigated by adding of its in the range of 25–150 mg. The results depicted in Fig. 5 show that 150 mg of the SiO_2@MNDs is the enough to reach maximum adsorption, completely elution and quantitative recoveries of Pb(II). Therefore, further studies were carried out by using 150 mg of SiO_2@MNDs as adsorbent.

The effect of vortex agitation time on adsorption of Pb(II) was studied in the range of 1–5 min, and the mixing time of 2 min was found to be sufficient to hold Pb(II) ions in the solution medium on the adsorbent. Same experiments were carried out for desorption of Pb(II) ions adsorbed on the sorbent, and 3 min of vortex agitation time was found to be sufficient for quantitative recovery of Pb(II).

Applicability of an analytical procedure for the real samples is mainly dependent on the sample volume since it reaches the lowest measurable concentration and obtains high enrichment factor and low detection limit [15, 35–40]. Hence, the influences of the sample volume on the recoveries of Pb(II) by using presented VAMSPE method were investigated in the sample volume ranging from 10 to 40 mL. The results are depicted in Fig. 6. The quantitative recovery values were obtained in the sample volume range of 10–20 mL. The obtained results showed that our method was applicable for maximum 20 mL of sample volume by using 150 mg of the SiO_2@MNDs. Hence, we used our VAMSPE method for analysis of lead in the cigarette and Bush Branches and Leaves samples.

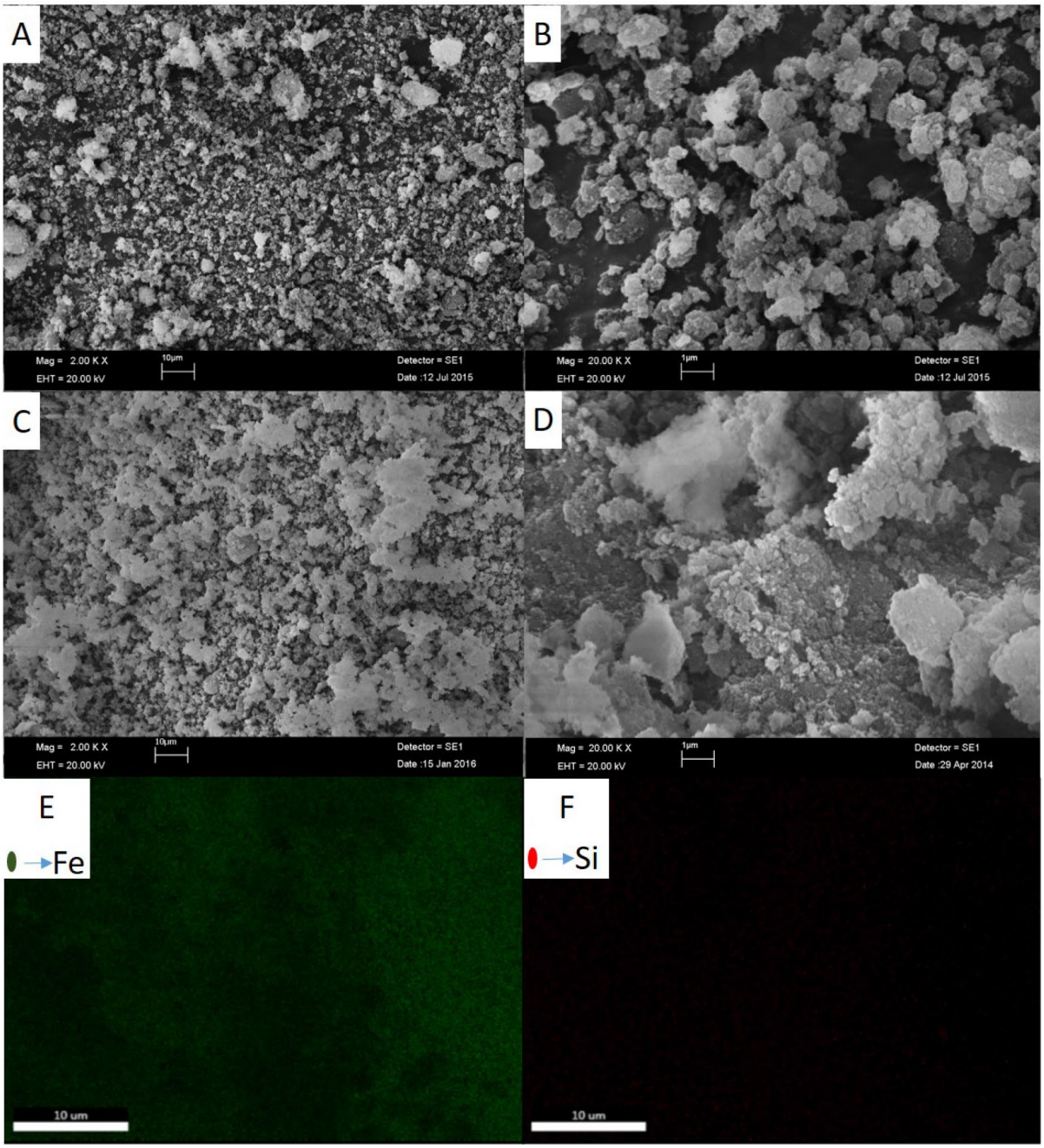


Fig. 3 SEM analysis of the pristine NDs **a**, **b** and SiO_2@Fe_3O_4@NDs **c**, **d** and EDX analysis of the pristine NDs and SiO_2@Fe_3O_4@NDs

Elution of lead(II) from SiO_2@MNDs could be done by using diluted mineral acids such as HCl and HNO_3. Therefore, for quantitative recovery of Pb(II) ion, the adsorption studies were conducted by using 1–3 M of hydrochloric acid and nitric acid solutions both in distilled water and acetone and moreover thiourea solution in 1–3 M HCl. The results given in Table 1 designate that quantitative recoveries of Pb(II) can be achieved by using 4% thiourea in 1 M HCl. Effect of eluent volume on the recovery of Pb(II) was studied in the range from 1.0 to 5.0 mL. The results given in Fig. 7 show that recovery of Pb(II) was increasing with increasing volume of eluent and reached quantitative value with 5.0 mL. Hence, 5.0 mL of 4% thiourea in 1 M HCl was selected as eluent for further experiments.

The number of cycles of the adsorbent used for adsorption studies was also optimized that each adsorbent can be used four times. It is because of partial dissolution of Fe_3O_4.

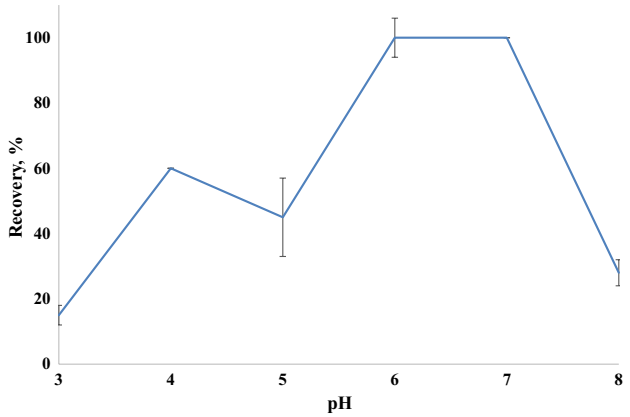


Fig. 4 Effect of pH on the % recovery of lead(II) (N:3)

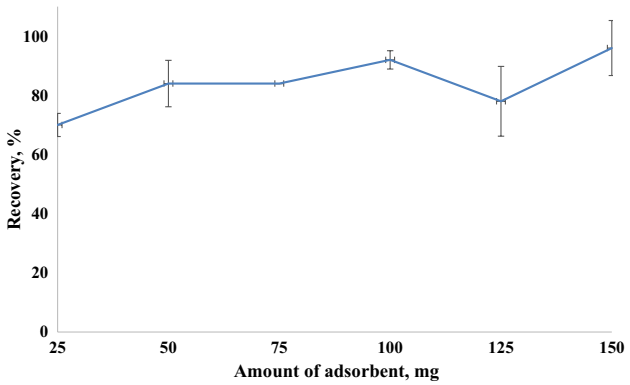


Fig. 5 Effect of the SiO_2@Fe_3O_4@NDs amount on the % recovery of lead(II) (N:3)

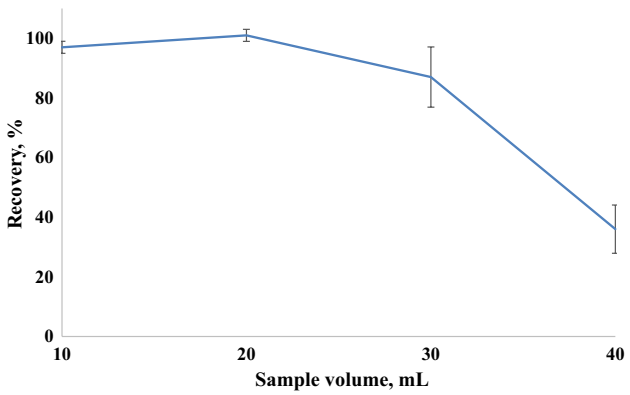


Fig. 6 Influence of volume of sample on the % recovery of lead(II) (N:3)

Therefore, SiO_2@MNDs were used four times for the rest of the other adsorption studies with 4 mL of 1 M HCl and 4% thiourea.

The effects of coexisting ions were studied on percent recovery of Pb(II). Table 2 shows that there is a negligible effect of these ions on percent recovery of Pb(II). The study

Table 1 Influences of eluent type on the recovery % of lead(II) (N:3)

Elution solution	Recovery %
2 M HNO_3	83 ± 2
3 M HNO_3	102 ± 3
2 M HCl	97 ± 2
3 M HCl	98 ± 1
4% thiourea in 1 M HCl	99 ± 1
4% thiourea in 2 M HCl	87 ± 6
4% thiourea in 3 M HCl	94 ± 6
3 M HNO_3 in 20% acetone	82 ± 6
3 M HNO_3 in 15% acetone	75 ± 6

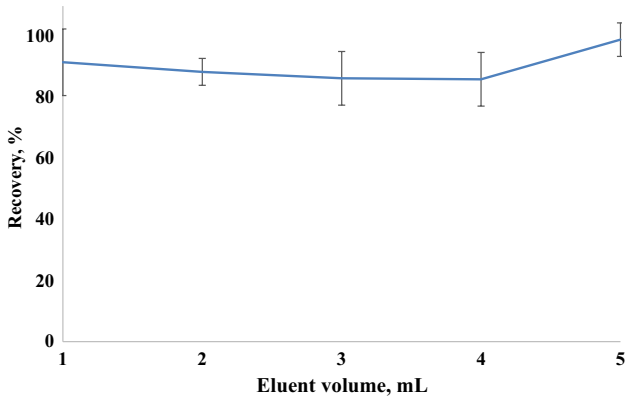


Fig. 7 Influence of volume of eluent on the % recovery of lead(II) (N:3)

Table 2 Effect of matrix ions on % recovery of lead(II) (N:3)

Matrix ions	Added as	Concentration, mg L^{-1}	Foreign ion/Pb(II)	Recovery %
Ca^{2+}	$Ca(NO_3)_2{\cdot}4H_2O$	1000	1500	88 ± 3
Na^+	$NaNO_3$	2500	3750	93 ± 3
Zn^{2+}	$Zn(NO_3)_2{\cdot}6H_2O$	10	15	95 ± 1
SO_4^{2-}	Na_2SO_4	1000	1500	97 ± 5
Mn^{2+}	$Mn(NO_3)_2{\cdot}4H_2O$	10	15	93 ± 1
Ca^{2+}	$Ca(NO_3)_2{\cdot}6H_2O$	1000	1500	88 ± 2
Cu^{2+}	$Cu(NO_3)_2{\cdot}3H_2O$	5	7.5	107 ± 1
K^+	KCl	2500	3750	103 ± 3
Mg^{2+}	$Mg(NO_3)_2{\cdot}6H_2O$	500	750	100 ± 3

shows that the solid-phase extraction of Pb(II) on SiO_2@MNDs is highly effective.

Analytical performance of the method

Some analytical characteristics of the presented method were studied. The preconcentration factor was calculated by dividing the highest sample volume by which the method

can be applied (20 mL) to the final volume (4 mL). Limit of detection (LOD) was found as 40.8 µg L^{-1} (3 Sb/m 3 Sb: three times of the standard deviation of 11-run measurements of blank solution and m: the slope of the calibration curve after extraction). Limit of quantification (LOQ) was found as 135 µg L^{-1} (10 Sb/m 10 Sb: ten times of the standard deviation of seven-run measurements of blank solution and *m*: slope of the calibration curve after extraction). The intra-day relative standard deviation was worked with applying the developed VAMSPE for analysis of 73349 Bush Branches and Leaves certified reference material and found as 5.3%. The inter-day relative standard deviation was worked by applying the developed VAMSPE for analysis of cigarette samples for different days and found as 11.1%. Calibration curve for Pb(II) is equal to $A = 0.0021C + 0.0001$ with $R^2 = 0.991$ (A: absorbance values obtained from FAAS and C: concentration of lead as mg L^{-1}).

Application of the method

For the validation of proposed method, the experiment was carried out for the determination of lead in NCSDC 73349 certified reference material as shown in Table 3. Recovery result shows that the method is accurate and valid for the determination of Pb(II) at trace level. The accuracy of the certified reference material results is verified by comparison, using a *t* test, of the certified value and found value. *t* critical value is 2.92 for 95% confidence level. The comparison shows that our method is true due to the similarity of the results.

For addition recovery, the method was applied to cigarette samples, and the recovery results are given in Table 4. The quantitative percent recovery in the range shows that method can be successfully applied to the determination of lead in the cigarette samples. The application of the method the certified reference material shows that the method is highly accurate and valid for the determination of Pb(II). In the developed VAMSPE method, the extraction of Pb(II) was carried out by using SiO_2@MNDs as an adsorbent. After validation experiments, the developed VAMSPE method was applied to different cigarette samples, and lead concentrations found are given in Table 5.

Table 3 Validation of the proposed VAMSPE method for Pb(II) at trace level NCSDC 73349 certified reference material (N:5)

Certified reference material	Pb(II)			
	Certified value mg/kg	Found value mg/kg	Recovery %	*t* value
NCSDC 73349	47 ± 3	48 ± 2	98	0.87

Table 4 Addition and recovery results for Pb(II) in cigarette sample using the proposed VAMSPE method (N:3)

Sample	Pb(II)		
	Added µg	Found µg	Recovery %
Cigarette	0	6.8 ± 0.6[a]	–
	5	11.1 ± 0.5	94
	10	17.9 ± 0.5	106

[a]Mean ± standard deviation

Table 5 Application of VAMSPE method to different cigarette samples (N:3)

Samples	Lead concentration µg g^{-1}
Cigarette I	UDL[a]
Cigarette II	9.4 ± 0.0
Cigarette III	8.4 ± 1.8

[a]Under detection limit

Table 6 Comparison of some methods in literature for determination of lead with the presented work

Technique	System	Instrument	Eluent	PF	Detection limit (µg L^{-1})	R.S.D. (%)	pH	References
CPE	Triton X-114; bis(1H-benzo[d] imidazol-2yl)ethyl)sulfone	FAAS	1.0 mol L^{-1} HNO_3 in methanol	39	2.8	2	8	[41]
SPE	Naphthalene/	FAAS	3.0 mol L^{-1} HNO_3	100	4.5	1–2.2	4	[42]
SPE	XAD-2/2-(2'-benzothiazolyazo)-p-cresol	FAAS	0.050 mol L^{-1} HCl	60	1.7	–	7–7.5	[43]
CPE	DDTP	FAAS	0.050 mol L^{-1} HCl	43	2.86	1.39	–	[44]
CoP	Manganese dioxide	ICP-OES	HNO_3/H_2O_2	20	3.2	< 5	3	[45]
CoP	Yttrium phosphate	ICP-AES	4.0 mol L^{-1} HNO_3	–	0.0137	–	3	[46]
CoP	Aluminum hydroxide	FAAS	4.0 mol L^{-1} HNO_3	125	16	< 9	7	[47]
VAMSPE	SiO_2@Fe_3O_4@NDs	FAAS	4 mL of 4% thiourea in 1 mol L^{-1} HCl	4	40.8	5.3	6	[Present work]

Comparison of the presented work with literature

The comparison of the presented solid-phase extraction procedure with the some preconcentration works in the literature is given in Table 6. The presented work is generally comparable with these methods with preconcentration factor, detection limit and RSD % values with some exceptions.

Conclusion

A new solid-phase extraction material (SiO_2@MNDs) is fabricated and characterized for the preconcentration–separation of lead(II) at trace levels prior to its flame atomic absorption spectrometric determination. The simple, rapid and accurate applicability are the main advantages of the proposed method. The effects of coexisting ions are at tolerable levels. The method was successfully applied to cigarette samples and NCSDC 73349 certified reference material for determination of lead at trace levels. In further studies, this new sorbent can be used for the extraction of different organic and inorganic species.

References

1. C. Koc, Environ. Prog. Sustain. Energy **37**, 1274–1284 (2018)
2. A.H. Dokmeci, T. Sabudak, V. Dalmis, Desalin. Water Treat. **148**, 213–221 (2019)
3. M. Krause, L.V. Vieira, T.P. Cunha, G.P. Brandão, P.R. Filgueiras, M. Tereza, W.D. Carneiro, J. Braz. Chem. Soc. **31**, 135–142 (2020)
4. A. Navas-Acien, E. Selvin, A.R. Sharrett, E. Calderon-Aranda, E. Silbergeld, E. Guallar, Circulation **25**, 3196–3201 (2004)
5. M. Yavuz, G. Çobanoğlu, J. Elementol. **24**, 1115–1128 (2019)
6. J.A. Arias, J.R. Peralta-Videa, J.T. Ellzey, M. Ren, M.N. Viveros, J.L. Gardea-Torresdey, Environ. Exp. Bot. **2**, 139–148 (2010)
7. M.G.A. Korn, G.L. Dos Santos, S.M. Rosa, L.S. Teixeira, P.V. De Oliveira, Microchem. J. **96**, 12–16 (2010)
8. Q. Zhou, N. Zhao, G. Xie, J. Hazard. Mater. **189**, 48–53 (2011)
9. M. Soylak, M. Koksal, Microchem. J. **147**, 832–837 (2019)
10. N. Altunay, A. Elik, R. Gürkan, Microchem. J. **147**, 49–59 (2019)
11. Y.K. Li, W.T. Li, X. Liu, T. Yang, M.L. Chen, J.H. Wang, Talanta **203**, 210–219 (2019)
12. J.Y. Kang, W. Ha, H. Zhang, Y.P. Shi, Anal. Methods **11**, 1735–1742 (2019)
13. M. Ramezanpour, S.N. Raeisi, S.A. Shahidi, S. Ramezanpour, S. Seidi, Anal. Biochem. **570**, 5–12 (2019)
14. M. Wierucka, M. Biziuk, TrAC Trends Anal. Chem. **59**, 50–58 (2014)
15. Q. Han, Z. Wang, J. Xia, S. Chen, X. Zhang, M. Ding, Talanta **101**, 388–395 (2012)
16. A. Ulu, S.A.A. Noma, S. Koytepe, B. Ates, Appl. Biochem. Biotechnol. **187**, 938–956 (2019)
17. C. Herrero-Latorre, J. Barciela-García, S. García-Martín, R.M. Peña-Crecente, J. Otárola-Jiménez, Anal. Chim. Acta **892**, 10–26 (2015)
18. J. Płotka-Wasylka, N. Szczepańska, M. de la Guardia, J. Namieśnik, TrAC Trends Anal. Chem. **77**, 23–43 (2016)
19. E. Yılmaz, M. Soylak, Talanta **158**, 152–158 (2016)
20. N. Baghban, E. Yilmaz, M. Soylak, J. Mol. Liq. **234**, 260–267 (2017)
21. S. Ulusoy, E. Yilmaz, Z. Erbas, H.I. Ulusoy, M. Soylak, Sep. Sci. Technol. (2020). https://doi.org/10.1080/01496395.2019.1623254
22. Z.A. Alothman, M. Habila, E. Yilmaz, M. Soylak, Microchim. Acta **177**, 397–403 (2012)
23. B. Shokri, M.A. Firouzjah, S.I. Hosseini, FTIR analysis of silicon dioxide thin film deposited by metal organic-based PECVD. in *Proceedings of 19th International Symposium on Plasma Chemistry Society*, Bochum, Germany, vol. 2631, (2009)
24. B. Alacakoc, Z. Tekin, T. Unutkan, G. Çetin, S. Bakirdere, At. Spectrosc. **40**, 233–237 (2019)
25. M.H. Morcali, A. Baysal, Int. J. Environ. Anal. Chem. **99**, 1397–1414 (2019). https://doi.org/10.1080/03067319.2019.1622695
26. L. Elci, M. Soylak, A. Uzun, E. Buyukpatir, M. Dogan, Fresenius J. Anal. Chem. **368**, 358–361 (2000)
27. K. Guclu, R, Apak. J. Colloid Interface Sci. **228**, 238–252 (2000)
28. N.K. Temel, R. Gürkan, J. Anal. Chem. **74**, 1174–1183 (2019)
29. M.A. Alheety, A. Raoof, S.A. Al-Jibori, A. Karadag, A.I. Khaleel, H. Akbas, O. Uzun, Mater. Chem. Phys. **231**, 292–300 (2019)
30. B. Hashemi, S. Rezania, Microchim. Acta **186**, 578 (2019). https://doi.org/10.1007/s00604-019-3668-2
31. W.I. Mortada, A.M. Abdelghany, Biol. Trace Elem. Res. **193**, 100–110 (2020). https://doi.org/10.1007/s12011-019-01704-8
32. H. Abdolmohammad-Zadeh, R. Mohammad-Rezaei, A. Salimi, Microchim. Acta **187**, 2 (2019). https://doi.org/10.1007/s00604-019-3937-0
33. S. Kahraman, N. Dogan, S. Erdemoglu, Int. J. Environ. Pollut. **34**, 275–284 (2008)
34. F. Armagan, M. Soylak, L. Elci, M. Dogan, J. Trace Microprobe Tech. **20**, 15–27 (2002)
35. Z. Dahaghina, H. Zavvar Mousavia, M. Sajjadia, F. Jahed, Scientia Iranica **25**, 3275–3287 (2018)
36. A. Ghiasi, A. Malekpour, Microchem. J. **154**, 104530 (2020). https://doi.org/10.1016/j.microc.2019.104530
37. B. Topuz, F. Kabadayi, A. Solmaz, Int. J. Environ. Anal. Chem. **99**, 641–652 (2019)
38. M.A. Kamboh, W.A.W. Ibrahim, H.R. Nodeh, L.A. Zardari, M.M. Sanagi, Environ. Technol. **40**, 2482–2493 (2019). https://doi.org/10.1080/09593330.2018.1444100
39. F. Shakerian, Y. Chelongar, A.M.H. Shabani, S. Dadfarnia, Microchem. J. **146**, 234–238 (2019)
40. M. Khan, J. Shah, M.R. Jan, Desalin. Water Treat. **173**, 274–282 (2020)
41. M. Ghaedi, A. Shokrollahi, K. Niknam, E. Niknam, J. Hazard. Mater. **168**, 1022–1027 (2009)
42. N. Pourrezza, R. Hoveizavi, Anal. Chim. Acta **549**, 124–128 (2005)
43. V.A. Lemos, J.S. Santos, L.S. Nunes, Sep. Sci. Technol. **40**, 1401–1414 (2005)
44. J.L. Manzoori, A.B. Tabrizi, Anal. Chim. Acta **470**, 215–221 (2002)
45. M.S. Bispo, E.S.B. Morte, M.G.A. Korn, L.S.G. Teixeira, M. Korn, A.C.S. Costa, Spectrochim. Acta Part B **60**, 653–658 (2005)
46. S. Kagaya, Y. Araki, N. Hirai, K. Hasegawa, Talanta **67**, 90–97 (2005)
47. G. Doner, A. Ege, Anal. Chim. Acta **547**, 14–17 (2005)